

# A simple algorithm for automated skin lesion border detection

P. TZEKIS\*, A. PAPASTERGIOU, A. HATZIGUIDAS, Z. ZAHARIS, D. KAMPITAKI, P. LAZARIDIS, M. GOULA\*\*

Department of Electronics

\*Department of Sciences - Faculty of Mathematics

\*\*Department of Aesthetics,

Alexander Technological Educational Institute of Thessaloniki,

57400 Thessaloniki,

GREECE

tzekis@tellas.gr, natp@el.teithe.gr, sakis@el.teithe.gr, zaharis@auth.gr,  
dimitra@her.forthnet.gr, pavloslazaridis@hotmail.com

*Abstract:* Prompt diagnosis is the most reliable solution for an effective treatment of melanoma. There is an ongoing research for providing computer-aided imaging tools in order to support the early detection and diagnosis of malignant melanomas. The first step towards producing such a diagnosis system is the automated and accurate boundary detection of skin lesion. Therefore, the present study introduces a new, simple, and very fast algorithm that has the ability to detect effectively and automatically the border of potential melanoma. The complexity of the proposed algorithm is  $O(\sqrt{N})$ , and thus the execution time, is dramatically minimized.

*Key-Words:* Melanoma, Dermatoscopy, ABCD rule, Image, processing, Border detection

## 1 Introduction

Early and accurate diagnosis is the most reliable solution for an effective treatment of melanoma [1,2]. Dermatoscopy has been established as a non invasive method to provide diagnostic support to dermatologists [3-5]. The best established dermoscopic diagnostic methods that have been set forth in the last few years are the ABCD rule of dermatoscopy, the Menzies method, the seven-point checklist, and pattern analysis [6-9]. Furthermore, there is an ongoing research worldwide to improve diagnostic accuracy of dermatologists by means of computer-based digital image analysis tools and methods [9-15]. Computer-aided methods have the ability not only to increase the diagnostic accuracy, but also to enable objectivity and repeatability [16-19].

The first step towards producing such a system is the automated and accurate boundary detection of skin lesion. Several image segmentation or boundary detection techniques are used by researchers for separating melanoma from normal skin. According to literature, some of these methods include region-based segmentation, adaptive

thresholding, k-means, fuzzy-c-means, SCT/center split, PCT/median cut, split and merge, multi-resolution segmentation, snake functions, radial search algorithms, etc.[20-29]. Nevertheless, automatic and accurate computer-aided boundary detection of lesion within reasonable time remains a challenging task. Edge detection must be efficient and reliable because it affects the validity, the efficiency and the subsequent computation of several shape and color features [20-30]. Therefore, the present work introduces a novel, simple and very fast algorithm, useful for the effective and automatic detection of melanoma border. The complexity of this algorithm is  $O(\sqrt{N})$ . In the following paragraphs, the proposed algorithm is described in detail.

## 2 Method Description

### 2.1 Automatic detection of skin lesion border

The first phase involves determining whether a point belongs to a melanoma, or not. Different melanoma images have different colors and contrasts. Hence, a “base” color between the color of the skin and the color of the melanoma must be calculated. This color can be defined by estimating the mean color of the image, using  $n^2$  calculations. In order to minimize the complexity of this process, the Monte Carlo method is applied with  $k$  points, resulting in a good approximation of the base color. The above-mentioned process is briefly described as follows:

Algorithm 1 (Calculation of the base color)

Step 1: Calculate the mean RGB color of the image, which is expressed as  $(mR, mG, mB)$ , where  $mR, mG,$  and  $mB$  are the mean values of Red, Green, and Blue colors, respectively.

Alternatively:

Step 1: Calculate the mean RGB color  $(mR, mG, mB)$  of  $k$  random points of the image.

Step 2: Return  $(mR + mG + mB) * coef$ , where  $coef$  is a parameter that determines how dark the points of the image must be in order to be considered as part of the melanoma ( Figure 1).

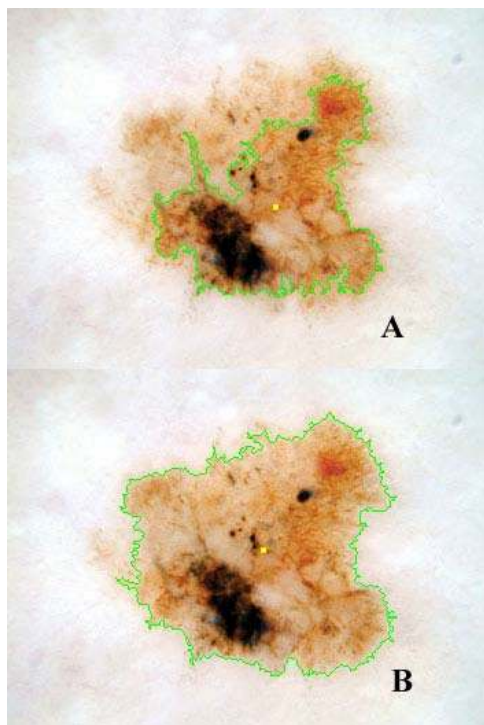


Figure 1. Resulted border detection using  
A:coef = 0.8 B: coef = 1

The second phase involves locating a random point inside the melanoma, either by searching the entire area of the image or by choosing random points around the center of the image.

We try to locate a  $(2k+1) \times (2k+1)$  square with all its points inside the melanoma. Should we decide to isolate a single dark point, we may select either a small black point or a hair on the image. Thus, we try to locate a compact area composed only of dark points, i.e., points whose color is darker from the base color.

An important fact to consider is that melanoma images may not have standard dimensions. The number  $k$  of points depends on the image size. The value of  $k$  should ideally vary between 4 and 10. In order to test whether the point  $(i,j)$  is accepted, we have to test all the points from  $(i-k, j-k)$  to  $(i+k, j+k)$ .

Another important issue is the selection of the right region of the melanoma. We suppose that the main region of the melanoma lies near the center of the image. Thus, the  $y$ -coordinate of the initial point is placed between  $cy/4$  and  $3*cy/4$  and the  $x$ -coordinate between  $cx/4$  and  $3*cx/4$ , where  $cx$  is the horizontal and  $cy$  is the vertical dimension of the image. The implementation of this algorithm is achieved by applying the Monte Carlo method.

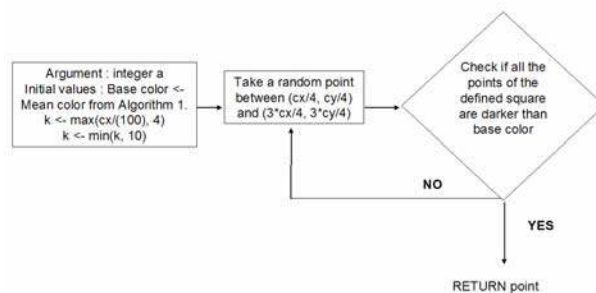


Figure 2. Flow chart of Algorithm 2 (Define a  $k \times k$  square so that all its elements are darker than the base color)

A flow chart of algorithm 2 is presented in Figure 2. Two example images and their estimated initial points (marked yellow) are shown in Figure 3.

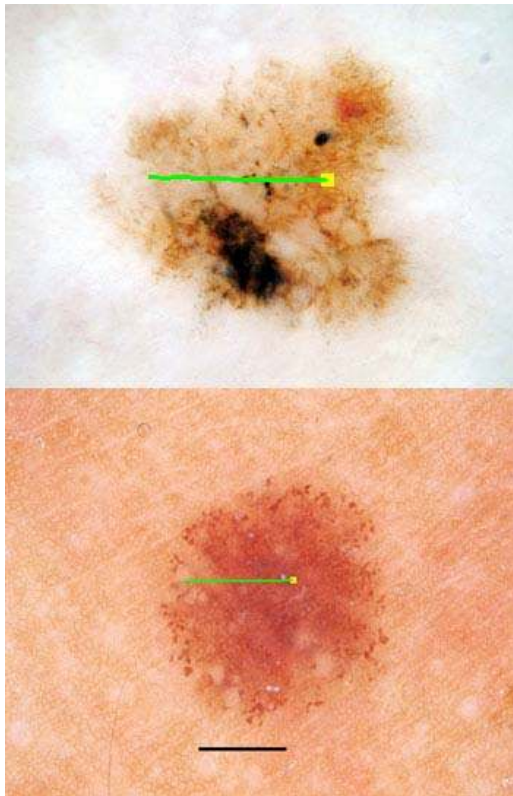


Figure 3. Execution of algorithm 3

In the next phase of the proposed algorithm we locate a point on the border of the melanoma. Starting from the initial point (point of reference), defined in the previous step, we test the left, up-left and down-left points with regard to the current point (Figure 4). Thus, a pixel that belongs to the melanoma can be identified by using the base color, which was calculated with algorithm 1 (Figure 3). The flow chart of algorithm 3 (Figure 5) describes this procedure in detail.

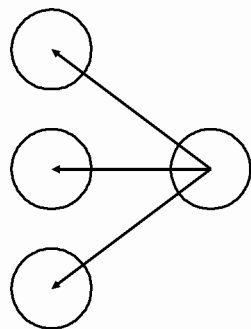


Figure 4. Finding the origin point

The results of algorithm 3 for the two melanoma images are represented in Figure 3. The green line stands for the algorithm process

for locating a point of lesion border, starting from the current point (yellow dot).

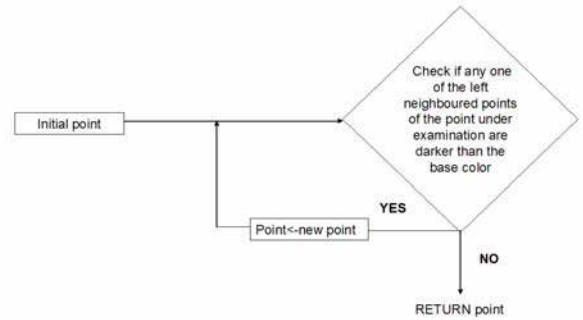


Figure 5. Flow chart of Algorithm 3 (point location on the melanoma border)

Once the previous processing is accomplished, we proceed with the main algorithm to define and draw the actual boundaries of the lesion.

The basic concept behind the algorithm is as follows:

Let  $(x,y)$  be the current and  $(x_0,y_0)$  be the previous point on the border of the melanoma. The next point  $(x_1, y_1)$  on the melanoma border is found by testing clockwise all the points around point  $(x,y)$  (Figure 6).

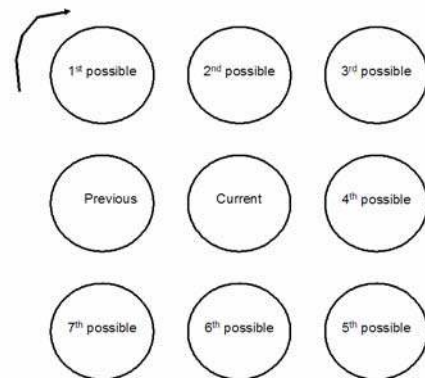


Figure 6. Execution of algorithm 4 for one pixel

Then, this point is added to the array of points and we set  $(x,y)=(x_1,y_1)$  and  $(x_0,y_0)=(x,y)$ . The algorithm terminates when we find a point very close to the first one.

The proposed algorithm is described in the following flowchart:



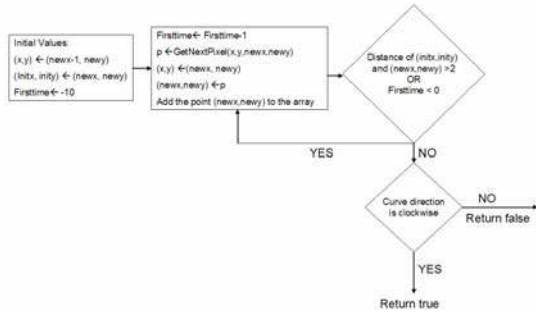


Figure 7. Flow chart of Algorithm 4 (Draw the border of the melanoma)

GetNextPixel function returns the next dark pixel according to the clockwise searching procedure as it is represented in Figure 6. In the end, Algorithm 4 checks whether the curve defines the actual lesion border or the border of a hole inside the skin lesion. To achieve this goal, the curve direction is examined. If the direction is clockwise the curve defines a melanoma border, otherwise the curve is the border of a hole inside the lesion (Figure 8). Because the algorithm stops when the distance value between the first point and the current point is less than 2, we use the variable “firsttime” to give 10 points in order to remove from the initial point.

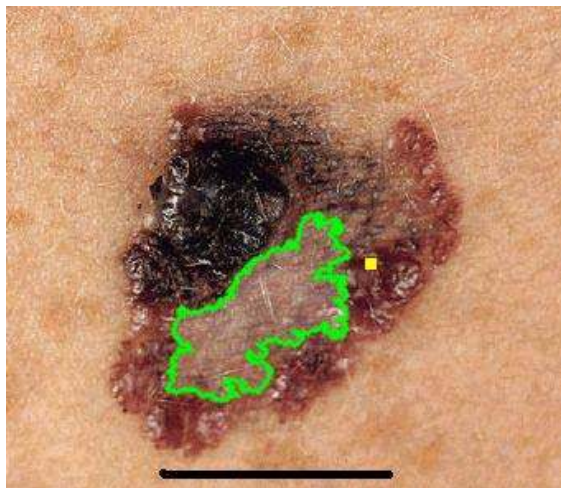


Figure 8. Instant failure of algorithm 4 since it defines the border of a hole inside the lesion

### 2.2 Hair removal algorithm

The presence of hair may result in a different lesion border than the actual one (Figure 9). Thus, a simple algorithm is employed to remove the hair that appears to cut the

borderline. For every n-th point of the defined border we check the next 15 points on the border one by one. If the Euclidian distance value between any (m-th) of these points and the n-th point is less than 3, then we remove all the points from the (n+1)-th point to the m-th one.

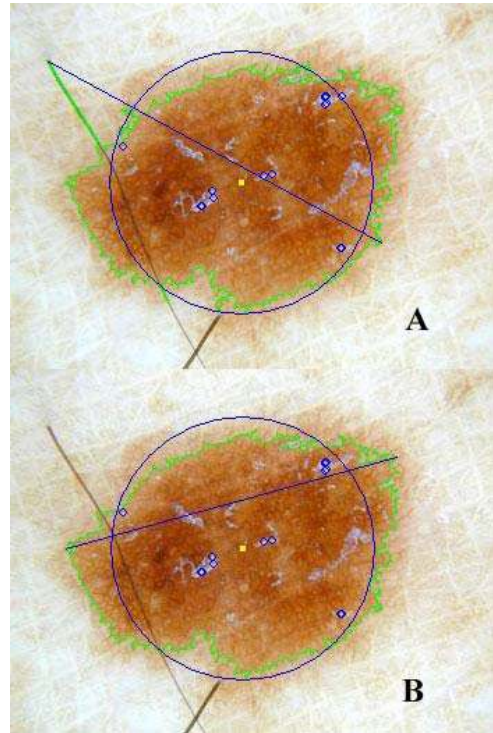


Figure 9. A: Hair presence is taken into account in the border detection B: Border detection after the application of hair removal algorithm

### 2.3 Overall algorithm

The overall procedure for automatic detection of melanoma border is actually accomplished by using all the above algorithms according to the flow chart shown in Figure 10.

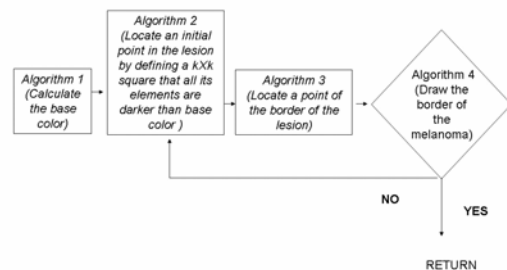


Figure 10. Flow chart of the proposed procedure

Using this procedure, the tumor area covered by melanoma can be accurately defined and its

extraction from the normal skin can be successfully accomplished. Assuming that the area of possible melanoma has been already accurately estimated, several meaningful features can be extracted.

The next section presents some examples of border detection using the proposed algorithm as well as the extracted image features.

### 3 Experimental results

#### 3.1 Implementation

The proposed boundary detection algorithm was implemented in the C programming language.

100 dermatoscopy images from a Tutorial CD were used in order to test the proposed boundary detection method [31].

##### 3.1.1 Feature calculation

Assuming that the region of skin lesion has been identified, meaningful features based on ABCD rule of dermatoscopy can be extracted from melanoma images by using simple mathematical calculations.

These features provide diagnostic support to doctors who apply the ABCD mnemonic diagnostic rule, and help them identify correctly the necessary diagnostic elements. In clinical medical practice, the ABCD mnemonic diagnostic rule must be combined with specific diagnostic criteria for each kind of lesion.

In this work, these features can provide an additional evaluation method by providing numerical values for comparison.

The features to be extracted from the images are A, B, C and D values that correspond to the ABCD mnemonic dermoscopic rule [6].

The ABCD rule of dermatoscopy is a well-established standard used in dermatoscopy analysis for classification of dermatological images to benign, suspicious or melanoma. ABCD stands for the following features: A = Asymmetry, B = Border, C = Color and D = Diameter or Differential structures [6,8].

According to literature, asymmetry is represented by different shape features (e.g., fragmentation index, circularity factor, asymmetry index) [20].

In order to describe the irregularity of the border, researchers use the thinness ratio, the circularity index and the variance of the

distance from the points of the lesion border to the centroid location [9,30].

The descriptors of color are mainly statistical parameters calculated from different color channels, like the average value and the standard deviation of the RGB or HSV color channels [9]. The presence of 6 basic colors inside the lesion gives 1 point for each color in order to calculate the C score (0-6 points) [6].

The patterns and structure of the lesion are of great importance. These characteristics include network, structureless areas, dots, globules, and streaks (0-5 points) [6,20]. Parameters for the description of dermatoscopic structures are hard to find in literature [25]. In some literature, the diameter of the lesion is estimated for D. If the diameter is larger than 6mm, the image can be stated as suspicious [5,30].

In the proposed approach, we choose four descriptors to represent the clinical features included in the ABCD rule, as follows:

1) derivation factor for Asymmetry 2) perimeter factor for Border 3) color presence for Color, and 4) the greatest diameter (in mm) of the lesion for Diameter.

Rule A - Derivation factor

The derivation factor is calculated by the following expression:

$$s^2 = \frac{\sum_{i=0}^n \left( \sqrt{(x_i - m_x)^2 + (y_i - m_y)^2} - r \right)^2}{(n-1)r}$$

where  $n$  is the number of points of the lesion border,  $r$  is the radius of the circle which has

the same area as that of the lesion,  $(m_x, m_y)$  is the center of gravity of the border and center of

the circle and finally  $(x_i, y_i)$  is the  $i$ -th point of the border.

The Asymmetry (A) of the lesion is evaluated by the Derivation Factor  $s$ . If  $s$  is close to zero, the lesion is almost a circle.

Rule B - Perimeter factor

Regarding border irregularities, the chosen descriptor is the Perimeter Factor, defined by:

$$P_f = \frac{n}{2\pi r}$$

where  $n$  is the number of points of the perimeter. When  $P_f$  is close to 1, the perimeter is considered to be «smooth».

### Rule C - Color

The presence of up to six colors i.e., white, red, light brown, dark brown, blue gray, and black, is considered. A 6×6 item table is defined. Each row contains the lower and upper limit RGB values that correspond to each of the 6 colors. The C score is increased by 1 point if there is at least one pixel inside the test region whose RGB values are between the upper and lower limit RGB values of any of the above-mentioned colors. Consequently, the C score varies from 0 to 6 and its actual value is shown on the right of the output image. Furthermore, the presence of any of the 6 colors is outlined on the output picture by small circles.

### Rule D – Diameter

For the sake of simplicity, in the present approach Rule D estimates the diameter. The diameter of the region is defined as the largest distance between the contour points of the region.

In order to determine the size of each lesion in mm, a 10mm black line is placed at the bottom of the melanoma image. A line is accepted if it is directed at most 45° from the horizontal direction. Then, a simple algorithm calculates the diameter of the melanoma in mm and represents the result on the output image.

### 3.1.2 Evaluation

Visual assessment was performed by expert dermatologists. The overall impression was very positive, as very good performance on both large and small skin lesions was achieved. It must be noted though, that a crucial constraint was that the tumor must be approximately centered within the field of view of the camera.

The results were very good even for skin lesions that had artefacts such as fuzzy skin lesion texture (Figure 8), hair (Figure 9) or ambiguous border (Figure 11). Additionally, the user has the opportunity to change the coef parameter (that determines how dark the points of the image must be in order to be considered as part of the melanoma) and the algorithm will detect a different border (Figure 1). Therefore, the expert dermatologist is able to choose the most preferable border of the skin lesion based on his experience.

Figure 11 presents some indicative results. The initial images are shown in the left column. The right column presents the output images where the lesion border was detected by applying the proposed algorithm. The detected border is coloured green.

Furthermore, for a set of 30 images, lesion borders were drawn by hand by a dermatologist. Figure 11 presents sample results. The lesion border (marked blue) drawn by an expert dermatologist is outlined in the middle column. Visual comparison between the border drawn by the dermatologist and of the automated extracted border by the proposed algorithm has been made. The estimated borders that resulted from the appliance of the proposed algorithm seem to resample the borders drawn by the dermatologist, but in a more detailed way.

After the detection of the lesion boundaries, the above-described procedures were applied in order to calculate the feature parameters, i.e., the derivation factor, the perimeter factor, the color presence, and the diameter of the lesion. The values of the feature parameters are presented on the lower right edge of each output image (Figure 11).

The ABCD values of the images that have been used from the CD have been already estimated and thus they can be used for comparison with the respective values calculated by the proposed algorithm. The accuracy of the detected boundaries resulted in acceptable values of the feature parameters as they have been evaluated by experts

According to literature, a boundary drawn manually by a dermatologist is usually subjective and so it cannot be used as an absolute reference. Nevertheless, it is a way to evaluate the accuracy of the boundaries provided by the proposed method compared to the opinion of an expert dermatologist [24].

Additionally, since there are many border detection methods for dermoscopy images in literature, it is necessary to compare the approach to other existing methods. However, most of them are rather complicated and difficult to implement from the beginning. For this reason, k-means algorithm was selected, an algorithm that is usually used for the detection of lesion boundaries and is reasonably straightforward.



The K-means algorithm and the proposed algorithm have been applied on a set of 30 dermatoscopic images from the Tutorial CD.

The results (Figure 12) outline that both algorithms detected similar border of skin lesions.

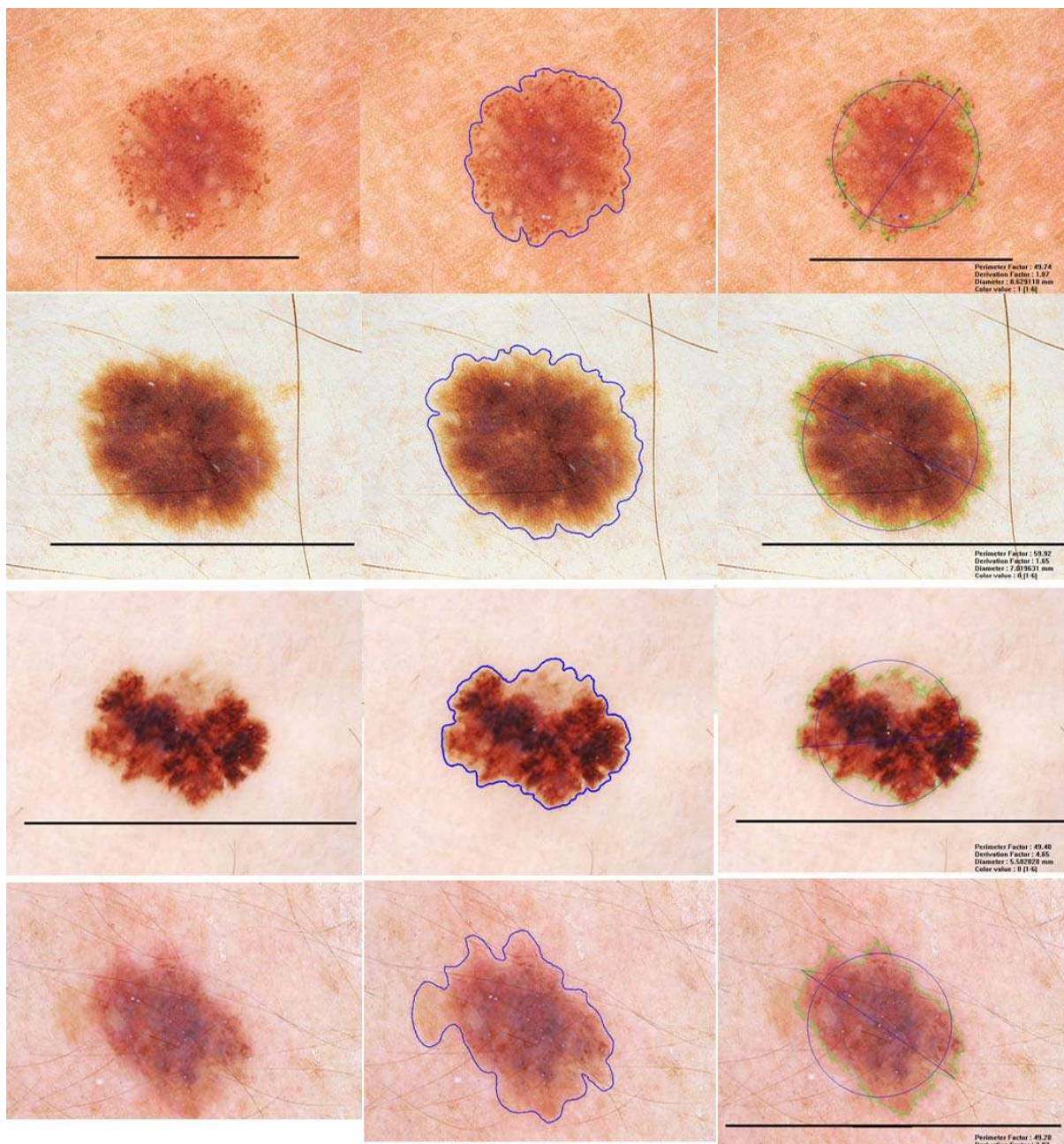


Figure 11. The left column presents the initial images. The middle column presents the lesion border (marked blue) drawn by an expert dermatologist and the right column presents the detected lesion border (marked green) using the proposed algorithm.

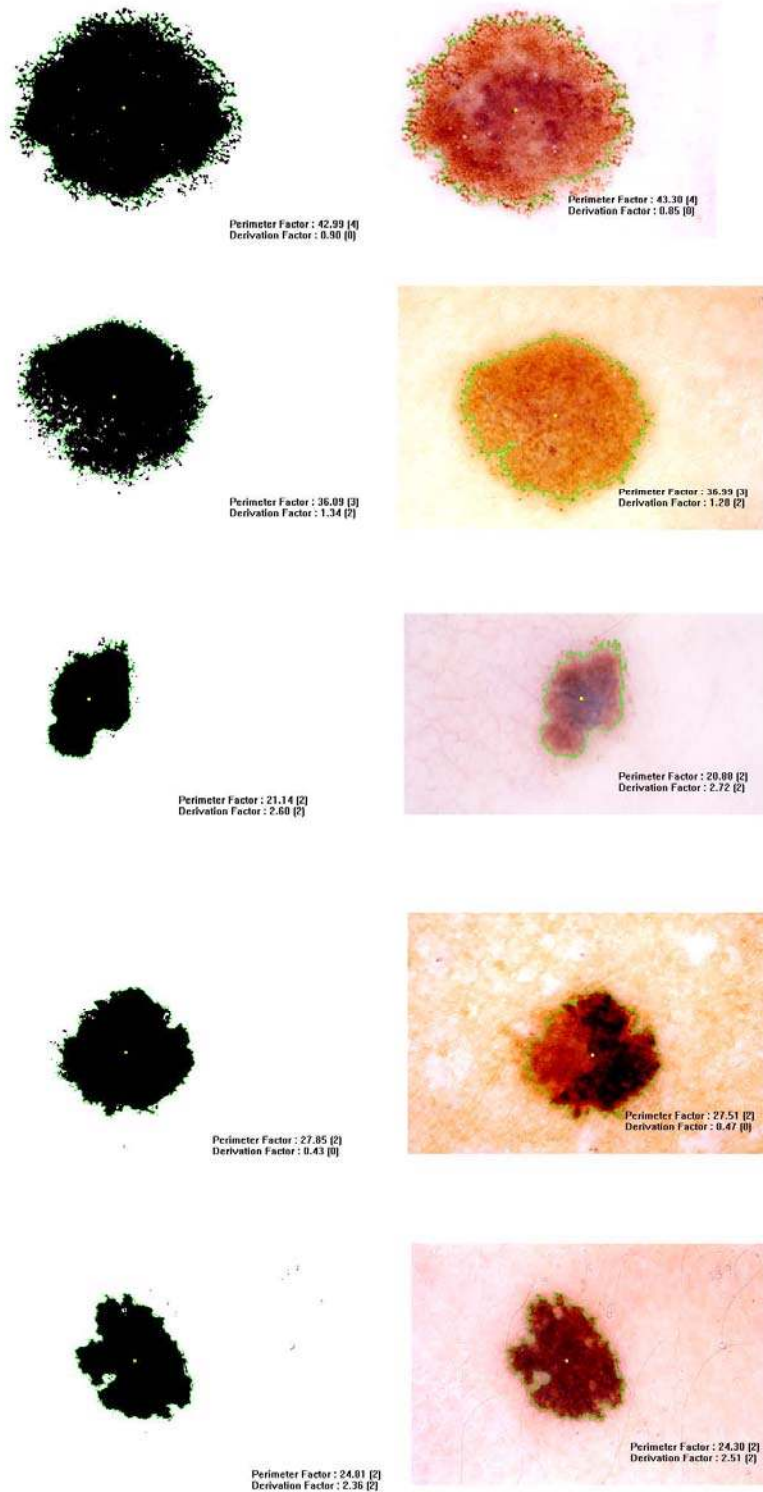


Figure 12. The left column presents the lesion border estimated by k-means algorithm and the right column presents the detected lesion border, using the proposed algorithm.



Table I: Perimeter - derivation factor according to k-means and proposed algorithm -statistical error.

A/A	Image Filename	Perimeter factor			Derivation factor		
		Proposed algorithm	k-means	Statistic error	Proposed algorithm	k-means	Statistic error
1	51.jpg	34,07	33,47	0,010756	3,15	3,23	0,001981
2	46.jpg	48,68	47,51	0,028813	4,18	4,28	0,002336
3	2.bmp	17,6	16,65	0,054204	0,91	0,77	0,025455
4	3.bmp	21,53	20,88	0,020235	1,38	1,31	0,00374
5	6.bmp	22,07	21,38	0,022268	1,48	1,54	0,002338
6	9.bmp	36,99	36,09	0,022444	1,28	1,34	0,002687
7	26.bmp	26,75	26,2	0,011546	1,37	1,44	0,003403
8	30.bmp	12,93	12,78	0,001761	0,47	0,48	0,000208
9	18.bmp	25,51	25,34	0,00114	0,34	0,33	0,000303
10	19.bmp	22,16	21,91	0,002853	0,49	0,52	0,001731
11	4.bmp	24,3	24,81	0,010484	2,51	2,36	0,009534
12	21.bmp	17,7	17,69	5,65E-06	2,41	2,43	0,000165
13	1.bmp	24,29	24,44	0,000921	2,44	2,1	0,055048
14	5.bmp	27,51	27,85	0,004151	0,47	0,43	0,003721
15	11.bmp	43,3	42,99	0,002235	0,85	0,9	0,002778
16	20.bmp	24,43	24,75	0,004137	4,16	3,89	0,01874
17	27.bmp	33,81	33,77	4,74E-05	1,59	1,63	0,000982
18	16.bmp	27,38	27,84	0,007601	0,94	0,75	0,048133
19	8.bmp	20,88	21,14	0,003198	2,72	2,6	0,005538
20	7.bmp	35,95	35,55	0,004501	4,18	4,77	0,072977
21	14.bmp	36,19	36,41	0,001329	6,69	6,36	0,017123
22	22.bmp	11,93	11,86	0,000413	0,39	0,35	0,004571
23	12.bmp	32,6	32,49	0,000372	1,04	0,96	0,006667
24	15.bmp	15,66	16	0,007225	4,46	3,87	0,089948
25	25.bmp	15,86	15,27	0,022796	0,35	0,48	0,035208
26	m5.jpg	29,4	31,81	0,182587	1,3	1,57	0,046433
27	me111	33,62	32,11	0,071009	2,82	2,92	0,003425
28	24.bmp	15,51	15,97	0,01325	2,5	2,37	0,007131
29	23.bmp	48,28	47,36	0,017872	7,02	8,07	0,136617
30	28.bmp	44,27	44,72	0,004528	10,42	10,12	0,008893
		<b>average error</b>		<b>0,00711</b>	<b>average error</b>		<b>0,008727</b>

For comparison reasons, numerical values based on Rule A and Rule B have been estimated.

The values that resulted from applying the proposed algorithm were compared to the corresponding values of applying the k means algorithm (reference standard) for the same images. The statistical error was defined by the following formula:

Statistical Error =  $(\text{proposed algorithm value} - \text{k-means value})^2 / \text{k-means value}$

Results are presented in Table I and in Figure 13 respectively.

The results do not reveal any significant differences between the values that were estimated for perimeter factor and derivation factor according to k-means and the proposed algorithm.

In conclusion, based on the results presented in this section, we can claim that our boundary detection algorithm performs as well as an expert dermatologist or k-means algorithm.

## 4 Discussion

A considerable interest has been shown in recent years in the development of computer-aided automated analysis of digitized dermoscopic images, that could diagnostically support dermatologists in the sensitive field of melanoma cases. The computation of lesion boundaries is the most important step in order to calculate subsequently several meaningful features. Accurate and fast automatic detection of melanoma border is a challenging task.

In this work we present a simple and effective algorithm for automatic detection of melanoma border. The algorithm aims to demarcate the tumor area from the surrounding skin and define the melanoma boundaries in detail.

The visual assessment and the statistical comparison described in the previous section pointed out the overall performance of the proposed algorithm.

An additional and very important advantage of the algorithm is the execution time. The complexity of

the proposed algorithm is  $O(\sqrt{N})$ , therefore it is faster than other similar algorithms. For example, an algorithm usually used for the detection of lesion boundaries is the k-means algorithm. The complexity of this algorithm is a polynomial in N ( $\Omega(N)$ ) and thus is greater than the complexity of our algorithm.

Provided that the melanoma consists of N points, the complexity of the algorithm is calculated as follows:

1. The estimation of the base color (Algorithm 1) needs  $3 \cdot k$  additions using the Monte Carlo method. Given that k is the integer part of  $\sqrt{N}$ , we finally need  $3 \times \text{Int}(\sqrt{N})$  additions.

2. In order to locate a point inside the melanoma (Algorithm 2) we need to test  $9 \times 9 = 81$  points and specifically 3 colors per point. Since we look at the image area between  $(cx/4, cy/4)$  and  $(3 \cdot cx/4, 3 \cdot cy/4)$ , i.e., one quarter of the image if the melanoma occupies the  $1/f$  of the image, the Monte Carlo method needs an average number of  $f/4$  points. Thus, we need  $9 \times 9 \times 3 \times f/4$  tests. Assuming that the size of the melanoma is bigger than  $1/8$  of the image, we need less than 486 ( $9 \times 9 \times 3 \times 8/4$ ) integer tests.

3. In order to estimate the border of the lesion (Algorithm 4), we need to test  $(p \times q)$  points  $\times 3$  colors per point, where p is the number of the points of the perimeter and q is the average number of tests per point, which is  $8/2 = 4$  (Figure 6). The number of points of the perimeter is proportional to  $\sqrt{N}$ . So, the number of tests we need in this algorithm is  $3 \times 4 \times \text{Int}(\sqrt{N}) = 12 \times \text{Int}(\sqrt{N})$ .

Finally, the total number of tests and additions we need is

$$3 \times \text{Int}(\sqrt{N}) + 486 + 12 \times \text{Int}(\sqrt{N}) = 15 \times \text{Int}(\sqrt{N}) + 486$$

which means that the complexity of the proposed algorithm is  $O(\sqrt{N})$ .

## 5 Conclusions

The proposed algorithm is fast, simple and accurate. Nevertheless, the performance of the whole procedure is expected to be evaluated by using a large number of images and by comparing the detected lesion boundaries and the estimated ABCD values with the corresponding results from expert dermatologists. It must be noted that the aim of digital melanoma image analysis is not to replace diagnosis by dermatologists but to provide supplementary diagnostic accuracy. Successful comparison will provide the guarantee of a reliable and effective algorithm that could be used as a

basis for the extraction and quantification of clinical features towards early diagnosis of melanoma.

#### References

- [1] T.L. Diepgen and V. Mahler, The epidemiology of skin cancer, *Br J Dermatol*, Vol 146, 2002, pp 1–6.
- [2] H. Koh, Cutaneous melanoma, *N Engl J Med*, Vol 325, 1991, pp 171–182.
- [3] G. Argenziano and H.P. Soyer, Dermoscopy of pigmented skin lesions—a valuable tool for early diagnosis of melanoma, *Lancet Oncol*, Vol 2, 2002, pp 443–449.
- [4] BA Zsolt, Dermoscopy (epiluminescence microscopy) of pigmented skin lesions. *Dermatol Clin*, Vol 15, 1997, 79–95.
- [5] Consensus Net Meeting on Dermoscopy <http://www.dermoscopy.org/>
- [6] W. Stolz, A. Riemann, A.B. Cagnetta et al., ABCD rule of dermatoscopy: a new practical method for early recognition of malignant melanoma, *Eur J Dermatol*, Vol 4, 1994, pp 521–527
- [7] S.W. Menzies, C. Ingvar, K. Crotty K and W. McCarthy, Frequency and morphologic characteristics of invasive melanomas lacking specific surface microscopic features, *Arch Dermatol*, Vol 132, 1996, pp 1178–1182.
- [8] H.R. Johr, Dermoscopy: Alternative Melanocytic Algorithms—The ABCD Rule of Dermoscopy, Menzies Scoring Method, and 7-Point Checklist, *Clinics in Dermatology*, Vol 20, 2002, pp 240–247
- [9] I. Maglogiannis and D. Kosmopoulos, Computational vision systems for the detection of malignant melanoma, *Oncology Reports special issue on Computational Analysis and Decision Support Systems in Oncology*, Vol 15, 2006, pp 1027–1033
- [10] A. Blum, H. Luedtke, U. Ellwanger, R. Schwabe, G. Rassner and C. Garbe, Digital image analysis for diagnosis of cutaneous melanoma. Development of a highly effective computer algorithm based on analysis of 837 melanocytic lesions. *British Journal of Dermatology*, Vol 15, No 5, 2004, pp 1029–1038
- [11] N. Cascinelli, M. Ferrario, R. Bufalino et al, Results obtained by using a computerised image analysis system designed as an aid to diagnosis of cutaneous melanoma, *Melanoma Res*, Vol 2, 199, pp 167–170
- [12] A. Green, N. Martin, J. Pfitzner, M., O'Rourke, N. Knight, Computer image analysis in the diagnosis of melanoma, *J Am Acad Dermatol*, Vol 31, 1994, pp 958–964.
- [13] J. Mayer, Systematic review of the diagnostic accuracy of dermatoscopy in detecting malignant melanoma, *Med J Aust*, Vol 167, 1997, pp 206–210.
- [14] H. Iyatomi, H. Oka, M. Hashimoto, M. Tanaka and K. Ogawa, K., An Internet-based Melanoma Diagnostic System - Toward the Practical Application, *Computational Intelligence in Bioinformatics and Computational Biology, CIBCB '05. Proceedings of the 2005 IEEE Symposium*, 2005, pp 1–4 <http://ieeexplore.ieee.org/iel5/10629/33563/01594952.pdf?arnumber=1594952>.
- [15] G. Grammatikopoulos, A. Hatzigaidas, A. Papastergiou et al, Simple Matlab Tool for Automated Malignant Melanoma Diagnosis, *WSEAS Trans. on Information Science and Applications*, Vol 3 No 4, 2007, pp 460–465.
- [16] B. Rosado, S. Menzies, A. Harbauer et al., Accuracy of computer diagnosis of melanoma: a quantitative meta-analysis, *Arch Dermatol*, Vol 139, 2003, pp 361–367.
- [17] G.R. Day and R.H. Barbour, Automated melanoma diagnosis: where are we at?, *Skin Research and Technology*, Vol 6, No 1, 2000, pp 1–5. <http://www.blackwell-synergy.com/doi/pdf/10.1046/j.1365-2133.2002.04978.x>
- [18] P.N. Hall, E. Claridge, J.D. Morris Smith, Computer screening for early detection of melanoma—is there a future?, *Br J Dermatol*, Vol 132, 1995, pp 325–338.
- [19] A. Horsch, W. Stolz, A. Neiss et al., Improving early recognition of malignant melanomas by digital image analysis in dermatoscopy, *Stud Health Technol Inform*, Vol 43, 1997, pp 531–535.
- [20] H. Ganster, P. Pinz, R. Rohrer, E. Wildling, M. Binder, H. Kittler, Automated melanoma recognition, *IEEE Transactions on Medical Imaging* Vol 20, No 3, 2001, pp 233–239.
- [21] GA Hance, SE Umbaugh, RH Moss, WV Stoecker, Unsupervised color image segmentation, *IEEE Eng. Med. Biol. Mag.* Vol 15, No 1, 1996, pp 104–111.
- [22] H. Iyatomi, H. Oka, M. Saito et al.: Quantitative assessment of tumor extraction from dermatoscopy images and evaluation of computer-based extraction methods for

- automatic melanoma diagnostic system, *Melanoma Res*, Vol 16 , 2006, pp 183–190.
- [23] B. Erkol, R.H. Moss, R.J. Stanley, W.V. Stoecker, E. Hvatum, Automatic lesion boundary detection in dermoscopy images using gradient vector flow snakes, *Skin Research and Technology* , Vol 11, 2004, pp 17–26.
- [24] P. Schmid, J. Guillod, J.P. Thiran, Towards a computer-aided diagnosis system for pigmented skin lesions, *Computerized Medical Imaging and Graphics*, Vol 27, 2003, pp 65–78.
- [25] Z. Zhang, W.V. Stoecker, R.H. Moss, Border detection on digitized skin tumor images, *IEEE Transactions on Medical Imaging*, Vol 19, No 11, 2000, pp 1128 -1143.
- [26] J.E. Golston, R.H. Moss, W.V. Stoecker, Boundary detection in skin tumor images: An overall approach and a radial search algorithm. *Pattern Recognition*, Vol 23, No 11, 1990, pp 1235–1247.
- [27] P.H. Schmid PH, Segmentation & symmetry measure for image analysis: application to digital dermatoscopy, *Thesis no. 2045, Swiss Federal Institute of Technology at Lausanne (EPFL), Signal Processing Laboratory (LTS)*; 1999, [http://ltswww.epfl.ch/pub\\_files/schmid](http://ltswww.epfl.ch/pub_files/schmid)
- [28] W.V. Stoecker and R.H. Moss, Digital imaging in dermatology, *Computerized Medical Imaging and Graphics*, Vol 16, No 3, 1992, pp 145-150.
- [29] L. Xu, M. Jackowski, A. Goshtasby et al, Segmentation of skin cancer images. *Image and Vision Computing*, Vol 17, 1999, pp 65-74.
- [30] A. Bono, S. Tomatis, C. Bartoli, G. Tragni, G. Radaelli, A. Maurichi, R. Marchesini, The ABCD system of melanoma detection: A spectrophotometric analysis of the asymmetry, border, color, and dimension. *Cancer*, Vol 85, 1999, pp 72-77.
- [31] Quizz Of Dermatoscopy, Pigmented skin tumors, Dr. Raoul Triller, *Hopital Franco-Britannique - Levallois - France La Roche-Posay, Laboratoire Pharmaceutique*, 2002.